Acta Med. Nagasaki 63: 11－25

Neuropeptide Y inhibits hepatocarcinogenesis in overnutrition in mice

Ayaka KINOSHITA[1], Hiroko HAYASHI[2], Natsuho KUSANO[2], Shun INOUE[2], Toshimitsu KOMATSU[2], Ryoichi MORI[2], Seongjoon PARK[2], Mitsuhisa TAKATSUKI[1], Susumu EGUCHI[1], Isao SHIMOKAWA[2]

[1] Department of Surgery, Nagasaki University School of Medicine and Graduate School of Biomedical Sciences, Nagasaki, Japan

[2] Department of Pathology, Nagasaki University School of Medicine and Graduate School of Biomedical Sciences, Nagasaki, Japan

Background: The incidence of hepatocellular carcinoma (HCC) with fatty liver disease has been increasing, and the sympathetic nervous system may be involved in hepatocarcinogenesis in such cases. Here we analyzed the impact of neuropeptide Y (Npy), which is released from sympathetic nerve endings, on hepatocarcinogenesis in different nutritional settings.

Methods: Hepatocellular carcinoma was induced by an intraperitoneal injection of diethylnitrosamine (DEN) in male C57BL6/J mice null for *Npy* gene ($Npy^{-/-}$) and their haplotype ($Npy^{+/-}$) as a control (Ctrl). The mice were subjected to one of three dietary regimens: *ad libitum* feeding with a standard diet (AL) or a high-fat diet (HFD), or 30% dietary-restricted feeding (DR).

Results: The occurrence and growth of HCC were accelerated in the $Npy^{-/-}$ mice, particularly in the AL and HFD conditions. Steatosis was promoted at 28 wks in the $Npy^{-/-}$ mice; steatohepatitis was not exacerbated in the $Npy^{-/-}$ mice at 28 or 48 wks. The alterations in the TNF*α*- and *IL*-6-mRNA expression levels and phosphorylated NF-*κ*B and ERK1/2 levels in the liver at 28 wks did not support the current paradigm of a steatohepatitis-HCC sequence. By contrast, the DR inhibited steatohepatitis and then hepatocarcinogenesis even in the $Npy^{-/-}$ mice, although the $Npy^{-/-}$-DR mice displayed peculiar findings, i.e., the activation of TNF*α*-NF-*κ*B signaling, a possible protective mechanism against the elevated cell proliferation and genotoxic stresses.

Conclusions: Npy exerts an inhibitory effect on the occurrence and growth of HCC, particularly in overnutrition. Npy is also dispensable for the tumor-inhibiting effect of DR. The activation of Npy could be a promising target for the prevention of HCC.

ACTA MEDICA NAGASAKIENSIA 63: 11－25, 2019

Key words: liver, neuropeptide Y (NpY), steatosis, hepatocellular carcinoma (HCC)

Introduction

The incidence of hepatocellular carcinoma (HCC) accompanied by non-alcoholic fatty liver disease (NAFLD) has been increasing in industrial nations.[1] NAFLD is one of the lifestyle-related diseases caused by a sedentary lifestyle with excess calorie intake, and NAFLD is thus associated with obesity. The involvement of the sympathetic nervous system (SNS) in not only the exacerbation of hypertension but also steatohepatitis in obese people is now recognized.[2,3] The SNS releases neuropeptide Y (Npy) as well as catecholamines.[3] In human NAFLD, catecholamines and Npy are increased and promote hepatic fibrosis via the activation of hepatic stellate cells.[4] The SNS was also reported to be activated in human cirrhotic liver, leading to a poor prognosis of HCC.[5] Experimental evidence suggest that the SNS promotes hepatocarcinogenesis via the activation of Kupffer cells.[5]

In contrast to overnutrition, a restriction of dietary calorie intake with essential nutrients, referred to as 'dietary restriction (DR),' reduces the incidence of cancers and extends the lifespan in laboratory rodents.[6] The lowered incidence of cancers is also confirmed in DR-fed monkeys,[7] implying the effectiveness of DR regimens in the prevention of cancers in

Address correspondence: Isao Shimokawa, Department of Pathology, Nagasaki University School of Medicine and Graduate School of Biomedical Sciences, 1-12-4 Sakamoto, Nagasaki 852-8523, Japan.
Tel.: +81-95-819-7051, Fax: +81-95-819-7052, Email: shimo@nagasaki-u.ac.jp

Received April 5, 2019; Accepted July 16, 2019

humans. We have reported that Npy is required for the full effects of DR; i.e., the inhibition of cancers and the extension of lifespan in mice.[8] We hypothesized that Npy and thus the SNS may play dimorphic roles in hepatocarcinogenesis in different nutritional conditions.

In the present study, we investigated potential roles of Npy in chemically induced hepatocarcinogenesis in three different nutritional settings: the *ad libitum* feeding of a standard diet (AL), the *ad libitum* feeding of a high-fat diet (HFD), and a DR regimen.

Materials and methods

Experimental animals and husbandry

The animal care and experimental protocols were approved by the Ethics Review Committee for Animal Experimentation at Nagasaki University. Since 2005, *Npy knockout* (−/−) mice and their control wild-type (WT) mice have been maintained on a mixed genetic background derived from intercrosses between $Npy^{-/-}$ (129S-Npytm1Rpa/J, Jackson Laboratory, Bar Harbor, ME, USA) and WT (129S6/SvEvTac, Taconic Farms, Germantown, NY) mice in a barrier facility at the Center for Frontier Life Sciences, Nagasaki University.[8]

In the present study, we mated male $Npy^{-/-}$ and female $Npy^{+/-}$ mice to generate $Npy^{-/-}$ and $Npy^{+/-}$ mice. A lifespan study indicated that a 30% DR regimen extended the lifespan and inhibited cancer in $Npy^{+/-}$ mice to the same extent as those in WT mice[8] (Suppl. Fig. S1, Suppl. Table S1). We therefore used Npy+/– mice as a control (*Ctrl*) group of mice versus $Npy^{-/-}$ mice.

Three male mice were housed in individual cages in the barrier facility (temperature 21°–24°C; 12-hr light-dark cycle) under specific pathogen-free conditions that were maintained for the entire study. All mice were fed *ad libitum* (AL) with a standard diet, i.e., Charles-River formula (CRF)-1 (Oriental Yeast Co., Tsukuba, Japan: 357 kcal/100 g) after weaning. The genotyping of mice was performed at 4 weeks of age (wks). When the mice were 12 wks old, we divided the mice into the AL, HFD (high-fat diet), and DR groups. The AL groups received the CRF-1 diet throughout the experiment. The HFD groups of $Npy^{-/-}$ and *Ctrl* mice were fed *ad libitum* with a high-fat diet (F2HFD1 diet, Oriental Yeast Co.: 414 kcal/100 g). The DR groups ($Npy^{-/-}$ and Ctrl) received a food allotment consisting of 70% of the mean daily intake of the CRF-1 chow in the $Npy^{-/-}$ and Ctrl groups, respectively every day at 30 min before the lights were turned off.

The food allotments for the DR groups were adjusted every 4 weeks between 12 and 40 weeks, and then the allotments were fixed. The details of the feeding procedure for the DR groups were as described.[8,9] The compositions of the CRF-1 and F2HFD1 diets are described in the Supplemental text, as are the food intake and body weight (BW) changes of the mice (Suppl. Fig. S2A–C).

Experimental design

Fifteen-day-old male mice received an intraperitoneal injection of DEN (25 mg/kg BW) for the initiation of hepatocarcinogenesis. For the analysis of hepatocyte proliferation, cell death, and DNA damage in *Ctrl* and $Npy^{-/-}$ mice after DEN injection, we collected liver tissues from each group of mice (n=4 or 5) at 48 hr post-DEN injection as described.[10] For the evaluation of the occurrence and growth of HCC, mice were sacrificed at 28 wks and 48 wks of age. Livers were excised and processed for histochemical analyses with a standard protocol, i.e., fixation in 4% paraformaldehyde overnight and paraffin-embedding. A part of each 28-wk tissue sample was quickly frozen in liquid nitrogen and stored at −80°C for biochemical analysis.

Histological analyses of HCC, steatosis, and steatohepatitis

We evaluated the occurrence of HCC in hematoxylin and eosin (H&E)-stained sections examined by light microscopy. HCCs that were <1 mm in dia. were designated as microscopic HCCs, and HCCs ≥1 mm in dia. were designated macroscopic HCCs. Hepatic steatosis was graded as a minimum (min; fatty change in hepatocytes <5%), moderate (mod; 5%–66.7% fatty change in hepatocytes), or severe degree (sev, fatty change in hepatocytes >66.7%) under a light microscopy examination of H&E sections. Steatohepatitis was evaluated in H&E sections as the density of inflammatory foci, in which neutrophils infiltrated mostly around fat droplets in hepatocytes. HCC areas and liver tissue areas in individual sections were measured using ImageJ 1.50g software (Wayne Rasband, National Institutes of Health, MD, USA) after images of H&E-stained sections were captured by a microscope equipped with a digital camera.

Immunohistochemistry, histochemistry, and immunofluorescence

To assess the cell proliferation and death of HCC cells, we performed an immunohistochemistry analysis with the antibody for proliferating cell nuclear antigen (PCNA; #MS-106-P0, Thermo Fisher Scientific, Cheshire, UK) in paraffin-embedded sections. Cell death was analyzed by TdT-mediated dUTP nick end labeling (TUNEL) histochemistry with a

commercially available kit (In situ Apoptosis Detection Kit, #MK500, Takara Bio, Shiga, Japan). DNA damage was assessed by immunohistochemistry with the antibody for γH2AX (#9718, Cell Signaling Technology, Danvers, MA). Steatohepatitis was also confirmed by immunofluorescence with antibodies for neutrophil (#ab2557, Abcam, Tokyo), α-smooth muscle actin (αSMA; #ab32575, Abcam), and F4/80 (#ab6640, Abcam) as described.[11]

Western blots for total protein abundance and the phosphorylated forms (p) of NF-kB, ERK1, and ERK2

Nuclear protein was extracted from liver tissues of 28-wk-old mice using NE-PER (Thermo Fisher Scientific, Waltham, MA) according to the manufacturer's instructions. The nuclear fraction was used for phosphorylated (p)-NF-κB and NF-κB detection. Whole tissue lysate was used for p-ERK1/2 and ERK1/2 detection. The details of the procedures are described in the Supplemental Text.

Detection of norepinephrine by ELISA

To determine the content of norepinephrine (NE) in the liver, we used frozen liver tissues maintained at −80°C with a norepinephrine enzyme-linked immunosorbent assay (ELISA) kit (Abnova, Taoyuan City, Taiwan). The NE-ELISA was performed according to the manufacturer's instructions. The details are provided in the Supplemental Text.

Quantitative real-time RT-PCR analysis

Total RNA was extracted from liver tissues (20 mg) with an RNeasy Mini kit and RNase-Free DNase Set (Qiagen, Tokyo) and quantified by spectrophotometry (NanoDrop, Wilmington, DE). Total RNA (500 ng) was reverse-transcribed using a ReverTra qPCR RT kit (Toyobo, Osaka, Japan). cDNA was diluted 50 times with EASY Dilution (TaKaRa Bio, Tokyo) before the polymerase chain reaction (PCR). The quantitative PCR was performed using Thunderbird SYBR qPCR Mix (Toyobo) according to the manufacturer's instructions. The details of the PCR with gene-specific primer sets for the mRNA of cytokines, Forkhead box O (FoxO)1 and nuclear factor, erythroid 2 like 2 (Nrf2) targets are described in the Supplemental Text.

Statistical analysis

The data that we obtained are expressed as the mean and standard error (SE) unless otherwise specified. We performed two- or three-factor (Genotype, Diet, Age) analyses of variance (ANOVA) and post hoc tests (Hsu-Dunnett or Tukey's honestly significant difference [HSD] tests) for the rate data analyses. The proportion data were analyzed using a logistic regression, chi-square, or Fisher's exact test. A p-value <0.05 was considered significant. All statistical tests were performed using JMP®Pro 13.0.0 software (SAS, Cary, NC).

Results

Hepatocyte proliferation, apoptosis, and DNA damage after DEN administration

To assess the possible effects of the loss of *Npy* gene on the DEN-induced genotoxic stress in mice, we measured the densities of PCNA+ cells, TUNEL+ cells, and γH_2AX+ cells immunohistochemically 48 hr after the administration of DEN to 15-day-old mice. Our observations demonstrated that the densities of all three cell types were not significantly different between the *Ctrl* and $Npy^{-/-}$ mice (Suppl. Fig. S3A–C).

Occurrence and growth of HCCs

In 28-wk-old mice, microscopic HCCs were found in six of the 12 (50%) *Ctrl*-AL mice, five of the 12 (41.7%) *Ctrl*-HFD mice, and one of the 12 (8.3%) *Ctrl*-DR mice (Table 1). The proportion of mice bearing an HCC was slightly but significantly increased in the $Npy^{-/-}$ mice compared to the *Ctrl* mice (logistic regression: Genotype, *Ctrl* vs. $Npy^{-/-}$, p=0.0426). The proportion of mice bearing HCCs was reduced in the DR groups compared to the AL and HFD groups (logistic regression: Diet, p=0.0195; DR vs. AL, p=0.0192; DR vs. HFD, p=0.0310). There was no significant difference in the presence of HCCs between the AL and HFD mice (p=0.8659).

Among the 48-wk-old mice, most had microscopic and/or macroscopic HCCs (Table 1). The proportion of mice with a macroscopic HCC was low in the DR groups compared to the other diet groups (p=0.0044 in *Ctrl* and $p<0.0001$ in $Npy^{-/-}$ when the data of the AL and HFD groups were combined, by Fisher's exact test; Table 1). There was no significant difference in the proportion of mice with a macroscopic tumor between the AL and HFD groups or between the *Ctrl* and $Npy^{-/-}$ mice (logistic regression: Diet, p=0.7200; Genotype, p=0.1141; Diet × Genotype, p=0.7993, when the DR data were eliminated). However, the HCC area density (i.e., the percentage of tumor areas in each liver tissue) was significantly greater in the $Npy^{-/-}$ mice compared to the *Ctrl* mice (Fig. 1A, two-factor ANOVA; Genotype, p=0.0001), particularly in the AL and HFD groups (Genotype

Table 1. Numbers of mice bearing hepatocellular carcinoma

		28 wk				48 wk			
		none	micro	macro	Total	none	micro	macro	Total
Ctrl	AL	6	6 (50.0%)	0	12	0	2	7 (77.8%)	9
	HFD	7	5 (41.7%)	0	12	1	2	6 (66.7%)	9
	DR	11	1 (8.3%)	0	12	0	8	1 (11.1%)[&]	9
$Npy^{-/-}$	AL	5	7 (58.3%)	0	12	0	1	11 (91.7%)	12
	HFD	4	8 (66.7%)	0	12	0	1	10 (90.9%)	11
	DR	8	4 (33.3%)	0	12	4	8	0 (0.0%)[$]	12

AL, mice fed ad libitum with the regular diet. DR, mice fed 30% less the regular diet, compared to AL mice. HFD, mice fed ad libitum with the high fat diet. none, no tumor. micro, hepatocellular carcinoma (HCC) less than 1 mm in diameter (area less than 0.785 mm^2). macro, mice with HCC greater than or equal to 1 mm in diameter. [&], p = 0.0044 (Fisher's exact test vs AL and HFD groups combined in the Ctrl mice at 48 wk. [$], p < 0.0001 (Fisher's exact test vs AL and HFD groups combined in $Npy^{-/-}$ mice at 48 wk).

× Diet, p=0.0012). Also, There was no significant difference between the *Ctrl*-DR and $Npy^{-/-}$-DR groups.

Following an earlier report,[12] we also analyzed the liver weight changes as an index of tumor growth (Fig. 1B). When we excluded the DR groups from the analysis, the liver weight was significantly greater in the $Npy^{-/-}$ mice compared to the *Ctrl* mice (three-factor ANOVA; Genotype, p=0.0116). We thus conclude that the loss of Npy promotes the occurrence and growth of HCC—in particular in the *ad libitum* and high-fat diet conditions—and that the long-term effect of the diet restriction regimen in mice without the Npy gene is the inhibition of HCC growth. Obviously, the loupe images of representative liver specimens of *Ctrl*-HFD and $Npy^{-/-}$-HFD groups in 48-wk-old mice (Figure 1C). Not only the size of livers as a whole but also HCCs in $Npy^{-/-}$-HFD mice are apparently larger than those of *Ctrl*-HFD mice.

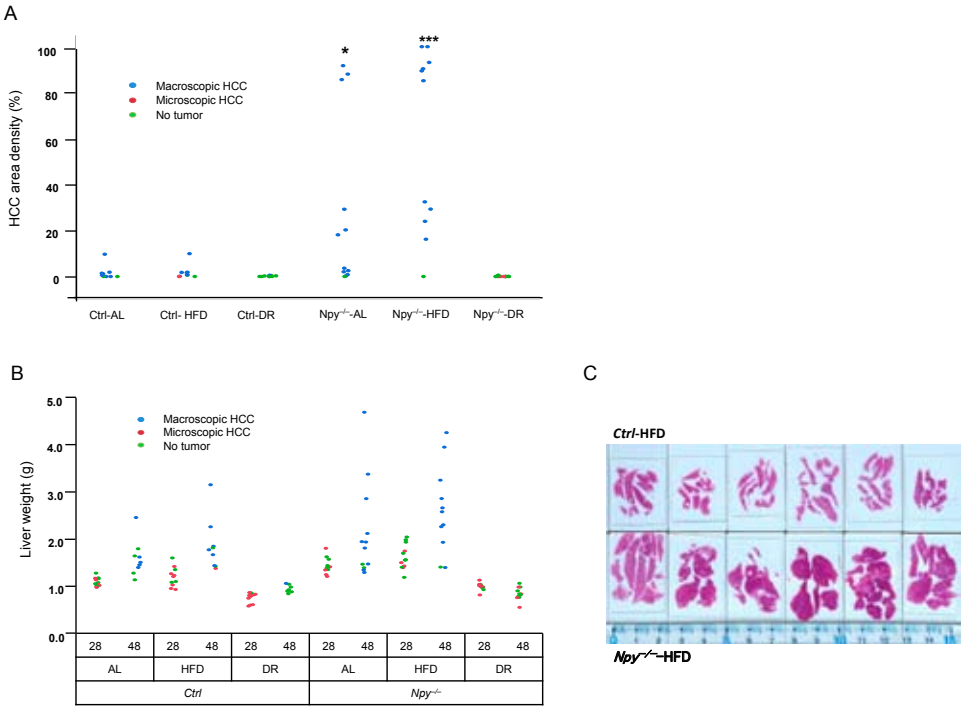

Figure 1. Growth of hepatocellular carcinomas (HCCs). **A:** The area density of hepatocellular carcinoma at 48 wks. The proportion of HCC-occupied area in the total area of liver tissue was plotted. *Ctrl*, control $Npy^{+/-}$mice. AL, the group of *ad libitum* feeding of the standard diet. HFD, the group of *ad libitum* feeding of the high-fat diet. DR, the group of 30% dietary-restricted feeding. Each point represents a mouse bearing no tumor (*green circles*), microscopic HCCs (tumor dia. <1. 0 mm, *red circles*), or macroscopic HCCs (tumor dia. ≥ 1.0 mm, *blue circles*). *Ctrl*-AL (n=9), *Ctrl*-HFD (n=9), *Ctrl*-DR (n=9), $Npy^{-/-}$-AL (n=12), $Npy^{-/-}$-HFD (n=11), $Npy^{-/-}$-DR (n=12). *p=0.0411 vs. *Ctrl*-AL. ***p=0.0002 vs. *Ctrl*-HFD. **B:** The liver weights in mice sacrificed at 28 and 48 wks. n=12 in each group at 28 wks. At 48 wks, *Ctrl*-AL (n=9), *Ctrl*-HFD (n=9), *Ctrl*-DR (n=9), $Npy^{-/-}$-AL (n=12), $Npy^{-/-}$-HFD (n=11), $Npy^{-/-}$-DR (n=12). **C:** Loupe images of livers in *Ctrl*-HFD and $Npy^{-/-}$-HFD groups at 48 wks. Livers are mostly occupied by masses of HCCs in $Npy^{-/-}$-HFD group, particularly 5 slides from the right.

Cell proliferation and death in HCC cells

Since the loss of Npy promoted the growth of HCCs, we evaluated the proliferation and apoptosis of HCC cells. Data for the *Ctrl*-DR mice at 28 wks were not available for statistical analysis because of the very low incidence of microscopic HCC in this group. When we analyzed the data of only the AL and HFD groups, the density of PCNA+ cells in HCCs was increased between 28 and 48 wks, particularly in the $Npy^{-/-}$ mice (Fig. 2A. two-factor ANOVA; Age, p=0.0097; Genotype × Age, p=0.0325; $Npy^{-/-}$-28 wks vs. $Npy^{-/-}$-48 wks, p=0.0002), but not in the *Ctrl* mice (*Ctrl*-28 wks vs. *Ctrl*-48 wks, p=0.9925). The density of PCNA+ cells in HCCs was significantly greater in the $Npy^{-/-}$-48 wks group than in the *Ctrl*-48 wks groups (p=0.0230). It should be noted that the density of PCNA+ cells fell significantly in the $Npy^{-/-}$-DR group between 28 and 48 wks (p<0.0001).

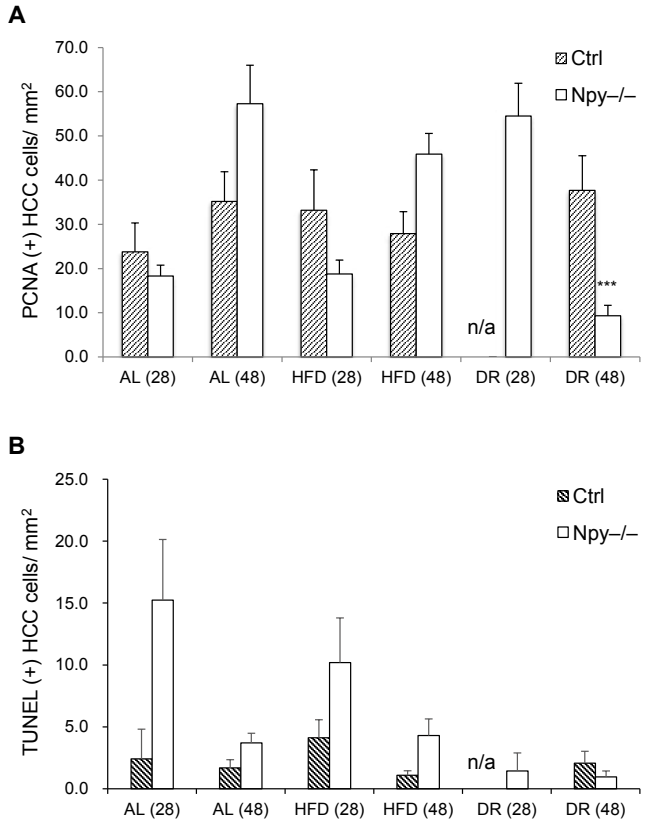

Figure 2. Cell proliferation and death in HCC cells. **A:** The density of PCNA+ HCC cells at 28 and 48 wks. Bars: mean ± SE. The number of images for the analysis in each group: 17 in *Ctrl*-AL (28 wks), 24 in *Ctrl*-AL (48 wks), 26 in $Npy^{-/-}$-AL (28 wks), 80 in $Npy^{-/-}$-AL (48 wks), 10 in *Ctrl*-HFD (28 wks), 58 in *Ctrl*-HFD (48 wks), 25 in $Npy^{-/-}$-HFD (28 wks), 76 in $Npy^{-/-}$-HFD (48 wks), n/a in *Ctrl*-DR (28 wks), 32 in *Ctrl*-DR (48 wks), 9 in $Npy^{-/-}$-DR (28 wks), 28 in $Npy^{-/-}$-DR (48 wks). ***p<0.0001 vs. $Npy^{-/-}$-DR (28 wks). **B:** The density of TUNEL+ HCC cells. Bars: mean ± SE (n=8–12 in each group). The number of images for the analysis in each group; 3 in *Ctrl*-AL (28 wks), 30 in *Ctrl*-AL (48 wks), 18 in $Npy^{-/-}$-AL (28 wks), 80 in $Npy^{-/-}$-AL (48 wks), 7 in *Ctrl*-HFD (28 wks), 60 in *Ctrl*-HFD (48 wks), 17 in $Npy^{-/-}$-HFD (28 wks), 79 in $Npy^{-/-}$-HFD (48 wks), n/a in *Ctrl*-DR (28 wks), 28 in *Ctrl*-DR (48 wks), 5 in $Npy^{-/-}$-DR (28 wks), 38 in $Npy^{-/-}$-DR (48 wks).

The density of TUNEL+ cells in the HCCs was decreased between 28 and 48 wks (Fig. 2B. three-factor ANOVA; Age, p=0.0018). When the data of the DR groups were excluded, the density of TUNEL+ cells was significantly greater in the $Npy^{-/-}$ mice compared to the *Ctrl* mice (Genotype, p=0.0042).

Steatosis and steatohepatitis

We evaluated steatosis and steatohepatitis in the liver as predisposing conditions of HCC.[1] At 28 wks, the proportion of mice with the minimum degree of steatosis was less in $Npy^{-/-}$ mice than in *Ctrl* mice (Genotype, p=0.0093, logistic regression; Fig. 3A), indicating that the loss of Npy promoted steatosis at 28 wks. The DR groups displayed significantly higher proportions of mice with minimum steatosis compared to the AL (p=0.0003) and the HFD groups (p<0.0001). There were no mice with severe steatosis in the AL groups, whereas most of the mice in the HFD groups showed severe steatosis. These results indicate that compared to the standard *ad libitum* diet, the diet restriction regimen inhibited steatosis and the high-fat diet exacerbated steatosis.

Steatosis was not significantly exacerbated in the *Ctrl* mice between 28 and 48 wks. Steatosis was attenuated in the $Npy^{-/-}$-HFD group but not significantly in the $Npy^{-/-}$-AL mice during this period (28 vs. 48 wks in the $Npy^{-/-}$-HFD mice, p=0.0373; 28 vs. 48 wks in the $Npy^{-/-}$-AL mice, p=0.1550; Fisher's exact test) (Fig. 3A). Thus, the loss of Npy promoted steatosis in the first half of the study period, but it attenuated rather than exacerbated steatosis in the latter half of the study period.

Neutrophils accumulated mostly around fat droplets in hepatocytes, representing steatohepatitis (Fig. 3B). In these foci, activated stellate cells that were positive for αSMA were also observed (Fig. 3C). At 28 wks, the density of inflammatory foci was significantly reduced in the DR groups compared to the AL and HFD groups (Diet, p=0.0003; DR vs. AL, p=0.0130; DR vs. HFD, p=0.0013; two-factor ANOVA) (Fig. 3D), and there was no significant difference between the AL and HFD groups (p=0.7163). The density of inflammatory foci in the $Npy^{-/-}$ mice did not differ from that in the *Ctrl* mice (Genotype, p=0.5757).

The density of inflammatory foci was significantly increased between 28 and 48 wks (Age, p=0.0117, three-factor ANOVA) (Fig. 3D). The density was significantly reduced in the DR

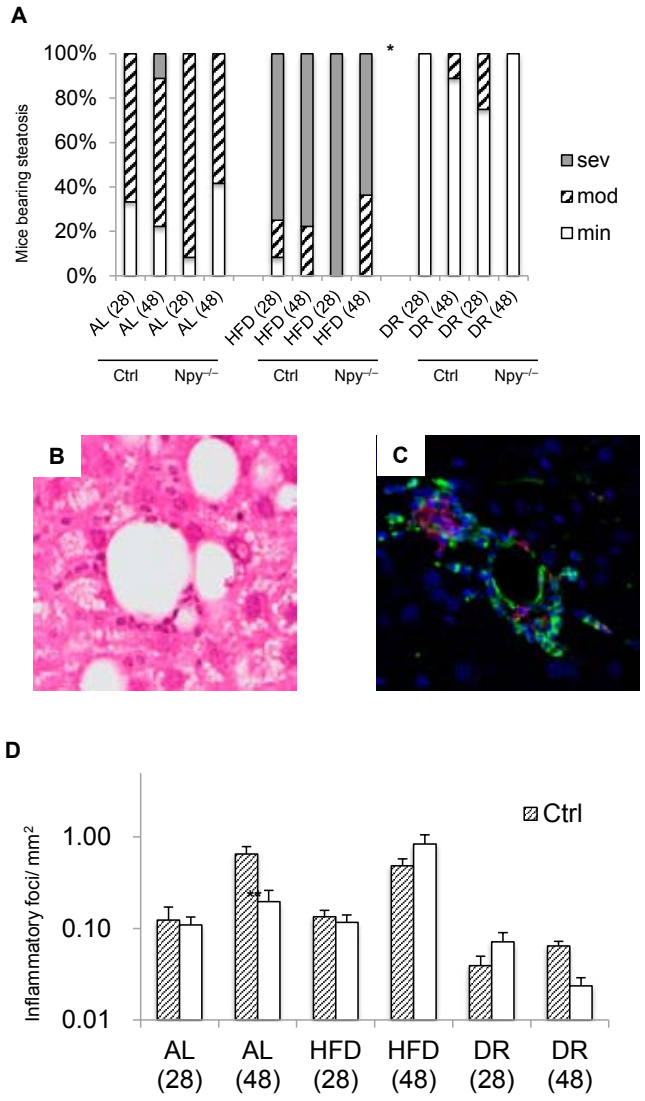

Figure 3. Steatosis and steatohepatitis. **A:** The proportion of mice bearing steatosis. Steatosis was graded as minimal (min; <5% fatty change in hepatocytes), moderate (mod; 5%–66.7%), or severe (sev; >66.7%). *p =0.0373 vs. *Npy*$^{-/-}$-HFD-28 wks by Fisher's exact test. The initial number of mice in each group was 12; at 48 weeks, n=9, 11, or 12 in each group. **B:** Steatohepatitis in H&E-stained sections (*Npy*$^{-/-}$-HFD at 48 wks). **C:** Immunofluorescence image of steatohepatitis. Neutrophils (green fluorescence surrounding a fat globule in the hepatocyte) and activated stellate cells (red fluorescence for αSAM) are also seen in the inflammatory focus. **D:** The density of inflammatory foci in the liver. Bars: mean ± SE (n=8–12, each group). **p=0.0175 vs. *Ctrl*-AL (48 wks).

groups compared to the AL and HFD groups (DR vs. AL, p<0.0001; DR vs. HFD, p<0.0001); the density was significantly greater in the HFD group compared to the AL group (p=0.0463). As a whole, the density of inflammatory foci was lower in the *Npy*$^{-/-}$ mice than in the Ctrl mice (Genotype, p=0.0323). At 48 wks, the density of inflammatory foci was significantly less in the *Npy*$^{-/-}$-AL mice compared to the *Ctrl*-AL mice (p=0.0175).

Histologic changes in mouse specimens at 48 wks, which are equivalent to the ballooning and Mallory-Denk body observed in human steatohepatitis (Figure 4). Since the ballooning and Mallory-Denk body, which represent cellular degeneration, often coexist in a microscopic area, we evaluated the severity of hepatocytic degeneration with those changes combined and scored 0, 1, and 2 (Figure 4A). When histologic changes were minimal but not zero, we decided to score 0.5. Figure 4B represents means of the scores and standard errors (n = 4 for each group). We also did a statistical analysis on the scores with two-factor ANOVA for the genotype and the diet and their interaction. The score could be greater in the *Ctrl* group than in *Npy*$^{-/-}$ group (Genotype, p = 0.0794); the score did not statistically differ among diet groups (Diet, p = 0.3776; Genotype × Diet, p = 0.8926).

Kupffer cells, which can be activated by steatosis, are involved in hepatocarcinogenesis.[5,13] In the present study, there was no histological evidence indicating that Kupffer cells were increased in the number in the *Npy*$^{-/-}$ mice

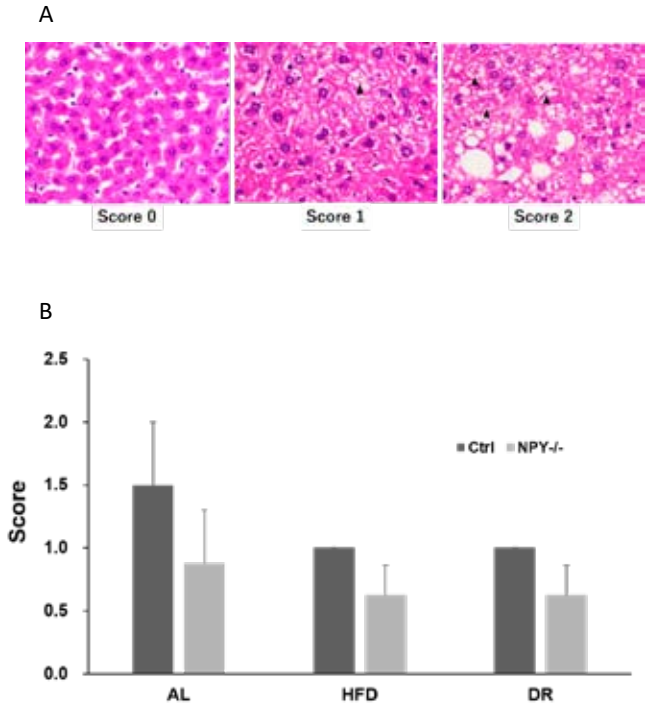

Figure 4. A: Severity of hepatocytic degeneration with ballooning of hepatocytes and Mallory-Denk body. Score 0, no finding. Score 1, ballooning of hepatocytes with a few Malory-Denk bodies (arrow head). Score 2, Ballooning of hepatocytes with a number of Mallory-Denk bodies (arrow head). Steatosis also coexists. **B:** Score of ballooning and Mallory-Denk body in the liver at 48 wks. The bars represent means + standard error (n = 4 in each group). The minimum histologic changes between Score 0 and Score 1, were scored as 0.5.

compared to the *Ctrl* mice (Suppl. Fig. S4).

Cytokines and related signaling

Increased levels of cytokines such as TNF-α and IL-6 and the activation or inhibition of cell signaling including the NF-κB and ERK pathways have been reported to be associated with hepatocarcinogenesis.[5,13-16] That type of signaling, if not all types, is activated in non-neoplastic liver tissues as well as HCC. We therefore measured the expression levels of *TNFα*- and *IL-6*-mRNA in the liver tissues at 28 wks. The *TNFα*-mRNA levels were significantly greater in the $Npy^{-/-}$ mice compared to the *Ctrl* mice (Genotype, p=0.0499, Fig. 5A), particularly in the DR groups (Genotype × Diet, p=0.0090, *Ctrl*-DR vs. $Npy^{-/-}$-DR, p=0.0069).

The *IL-6*-mRNA expression levels were also significantly higher in the $Npy^{-/-}$ mice compared to the *Ctrl* mice, particularly in the AL condition (Genotype × Diet, p=0.0013; *Ctrl*-AL vs. $Npy^{-/-}$-AL, p=0.0426, Fig. 5B). The *IL-6*-mRNA levels in the $Npy^{-/-}$-HFD mice did not differ from those in the *Ctrl*-HFD mice (p=0.1051). These data indicate a deregulation of the expression of inflammatory cytokines in $Npy^{-/-}$ mice even at baseline compared to *Ctrl* mice, although this appears to be dependent on the dietary regimens. However, there was no correlation between the degree of steatohepatitis and the cytokine expression levels (Suppl. Fig. S5A,B).

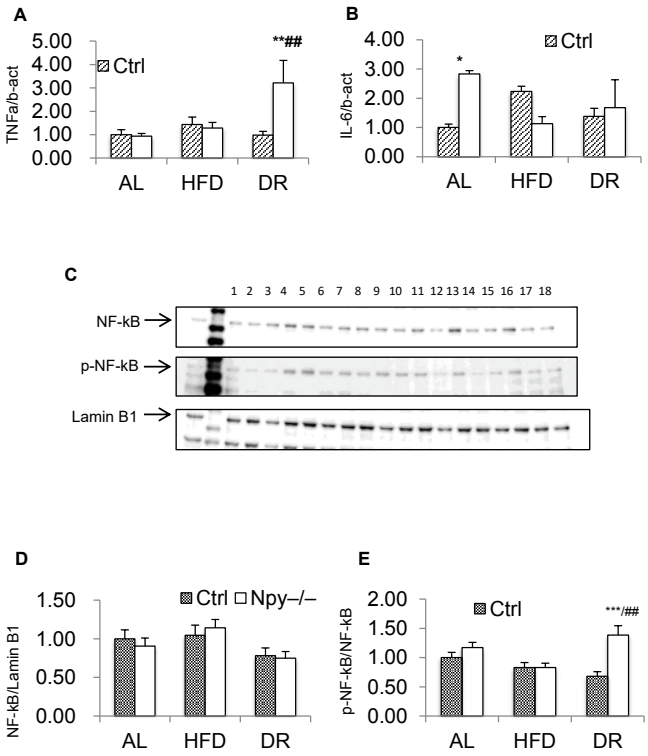

Figure 5. Cytokine mRNA expression and NF-κB protein abundance in the liver at 28 wks. **A:** The *TNFα*-mRNA levels normalized by *β-actin*-mRNA. Bars: mean ± SE (n=5, each group). **p=0.0069 vs. *Ctrl*-DR, ##p=0.0055 vs. $Npy^{-/-}$-AL. **B:** The *IL*-6-mRNA levels normalized by *β-actin*-mRNA. Bars: mean ± SE (n=5, each group). *p=0.0426 vs. *Ctrl*-AL. **C:** Immunoblotting of NF-κB p65, p-NF-κB p65, and lamin B1 in the nuclear fraction. Lanes 1-6: *Ctrl*-AL, *Ctrl*-DR, *Ctrl*-HFD, $Npy^{-/-}$-AL, $Npy^{-/-}$-DR, and $Npy^{-/-}$-HFD. Lanes 7-12 and Lanes 13-18 also represent samples of the groups, in the same order. **D:** The protein abundance of NF-κB normalized by lamin B1. Bars: mean ± SE (n=12, each group). **E:** The ratio of p-NF-κB to NF-κB. ***p<0.0001 vs. *Ctrl*-DR. ##p=0.0032 vs. $Npy^{-/-}$-HFD.

We measured the hepatic nuclear protein abundance of NF-κB and its active form, phosphorylated (p)-NF-κB at 28 wks (Fig. 5C). The protein level of NF-κB in the nucleus was significantly lower in the DR groups than in the HFD groups (Diet, p=0.0139; DR vs. HFD, p=0.0102; two-factor ANOVA) (Fig. 5D); there was no significant difference between the *Ctrl* and $Npy^{-/-}$ mice. The ratio of p-NF-κB to NF-κB was significantly higher in the $Npy^{-/-}$-DR mice compared to the *Ctrl*-DR mice (p<0.0001, Fig. 5E). Thus, the NF-κB pathway could be activated in the $Npy^{-/-}$-DR mice at 28 wks. The ratio did not differ between the *Ctrl* and $Npy^{-/-}$ mice when the data of the DR groups were excluded from the analysis.

The protein abundance of ERK1 normalized by β-actin did not differ among the mouse groups (Fig. 6A,B). Compared to the AL groups, the abundance of ERK2 was significantly reduced in the HFD groups (Diet, p=0.0113; AL vs. HFD, p=0.0092; two-factor ANOVA) (Fig. 6C). The ratio of p-ERK1 and ERK1 and that of pERK2 and ERK2 did not differ between the *Ctrl* and $Npy^{-/-}$ mice (Fig. 5D,E), although the HFD feeding decreased those levels compared to the AL group (Diet, p=0.0117; AL vs. HFD, p=0.0090 for p-ERK1/ERK1; p=0.0029 for p-ERK2/ERK2; two-factor ANOVA).

Effects on the sympathetic nervous system

The loss of Npy may affect the synthesis of norepinephrine (NE) and/or it secretion and/or the receptor expression levels. We therefore measured the tissue contents of NE and the expression levels of the subtypes α- and β-adrenergic receptor (Adr) mRNA in the liver. The NE content did not differ significantly between the *Ctrl* and $Npy^{-/-}$ mice (Fig. 7A). The mRNA expression levels of *Adrα1*, *Adrβ1*, and *Adrβ2* did not differ between the *Ctrl* and $Npy^{-/-}$ mice (Suppl. Fig. S6A-C). The diets also did not affect those expression levels. The *Adr3β*-mRNA expression levels did not differ significantly between the *Ctrl* and $Npy^{-/-}$ mice

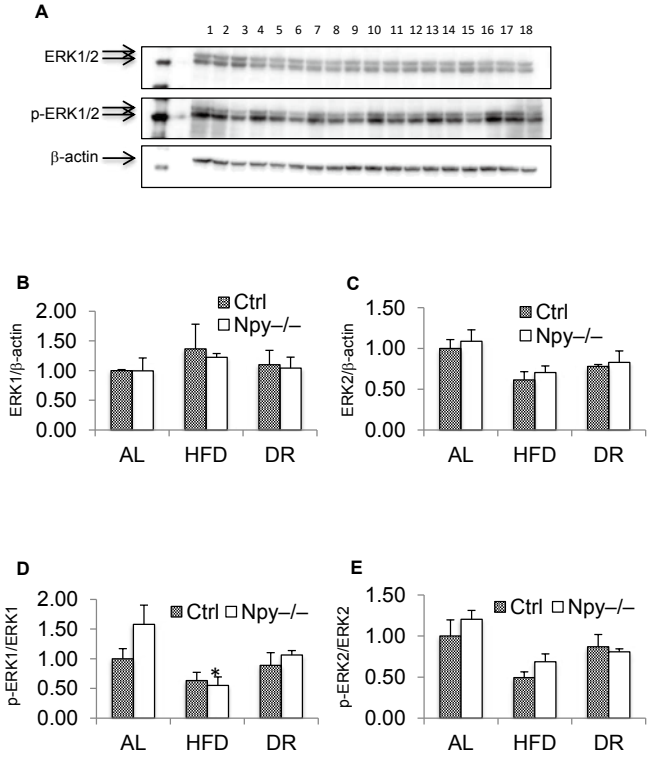

Figure 6. The protein abundance of ERK in the liver of mice at 28 weeks of age. **A:** Immunoblotting of ERK1 and ERK2 (ERK1/2), p-ERK1/2, and β-actin in the total cell lysate. Lanes 1-6: *Ctrl*-AL, *Ctrl*-DR, *Ctrl*-HFD, $Npy^{-/-}$-AL, $Npy^{-/-}$-DR, and $Npy^{-/-}$-HFD. Lanes 7-12 and Lanes 13-18 also represent samples of the groups, in the same order. **B:** The protein abundance of ERK1 normalized by β-actin. Bars: mean ± SE (n=3, each group). **C:** The protein abundance of ERK2 normalized by β-actin. Bars: mean ± SE (n=3, each group). **D:** The ratio of p-ERK1 to ERK1. Mean ± SE, n=3, each group; *p=0.0246 vs. $Npy^{-/-}$-AL. **E:** The ratio of p-ERK2 to ERK2. Mean ± SE, n=3, each group.

(Fig. 7B). The expression levels were upregulated by the high-fat diet compared to the *ad libitum* diet and diet restriction (Diet, p=0.0007; AL vs. HFD, p=0.0123; HFD vs. DR, p=0.0007; two-factor ANOVA). There was no significant difference in the expression levels between the AL and DR groups.

Gene expression

Two transcription factors—FoxO1 and Nrf2—which induce protective mechanisms against reactive oxygen species (ROS) and/or inflammatory stimuli in the liver are reported to be involved in the anti-tumor effect of dietary restriction.[9,17] We therefore analyzed the expressions of selected genes transcriptionally regulated by FoxO1 and/or Nrf2. Our analyses revealed that five of seven genes were differentially regulated between *Ctrl* and $Npy^{-/-}$ mice (Suppl. Fig. S7A-G). Of those genes, the mRNAs of the FoxO1 target genes *p21* and *p27* and *Sod2*-mRNA were upregulated in the $Npy^{-/-}$ mice, particularly in the AL group (*p21*: Genotype × Diet, p=0.0317; *p27*: Genotype, p=0.004; Diet, p=0.0119: *Sod2*: Genotype, p=0.0448; two-factor ANOVA). There were no significant alterations in the expression level of *Gadd45α*. These findings indicate that the loss of Npy promotes the activation of FoxO1 in the liver even at baseline, although the activation is dependent on the nutritional conditions.

Among the Nrf2 target genes, *Hmox-1*-mRNA was upregulated in the $Npy^{-/-}$ mice as shown in Suppl. Figure S7E (Genotype, p=0.0015, two-factor ANOVA). The high-fat diet also elevated the expression level (HFD vs. AL, p=0.0367; AL vs. DR, p=0.0165). By contrast, *Nqo1*-mRNA was down-regulated in the $Npy^{-/-}$ mice (Genotype, p=0.0280, two-factor ANOVA). The diet restriction elevated the expression levels. The Gclc-mRNA levels did not differ between the $Npy^{-/-}$ and *Ctrl* mice. The mRNA levels were significantly elevated in the AL groups compared to the HFD (p=0.0002) and DR groups (p=0.451).

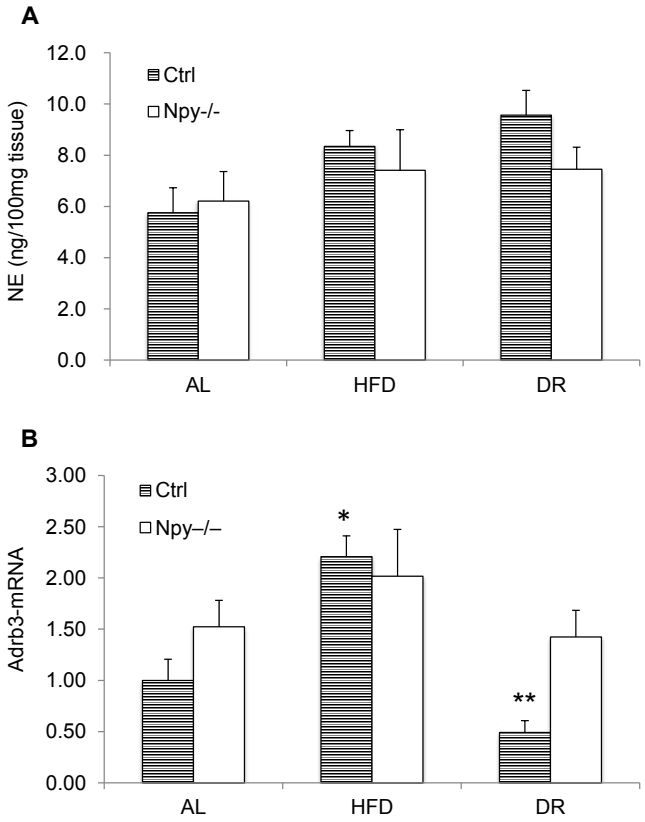

Figure 7. Effects of the loss of Npy on the sympathetic nervous system in the liver. **A:** The tissue content of norepinephrine (NE). Bars: mean ± SE (n=5 or 6, each group). **B:** The mRNA level of adrenergic receptor β3 (*Adrβ3*). Bars: mean ± SE (n=6, each group). *p=0.0458 vs. *Ctrl*-AL, **p<0.0017 vs. *Ctrl*-HFD.

Discussion

The results of this study demonstrate that the deficiency of Npy promotes the occurrence and growth of HCC, particularly in the *ad libitum* and high-fat diet conditions, supporting a role for the SNS in hepatocarcinogenesis in conditions of overnutrition. We observed that the loss of Npy elevated the proliferation rate of HCC cells between 28 and 48 wks; this effect was minimized in the control mice. Our findings suggest an inhibiting role for Npy in the proliferation of HCC cells. Indeed, in human HCC, Npy Y1 receptor (Npy1r) signaling is reported to significantly inhibit cell proliferation and the tumor growth.[18] In contrast, our present observations of TUNEL+ cells do not support the experimental paradigm that a reduction of apoptosis of neoplastic cells promotes the growth of HCC.

Npy counterbalances the actions of NE in several physiologically stressed conditions.[3] In an Npy-overexpressing rat model, Npy reduced sympathetic signals at baseline and diminished the immediate sympathetic response to stress.[19] Npy was also reported to attenuate stress-induced bone loss through a suppression of NE circuits.[20] Those findings indicated a counteracting role for Npy over NE in the activation of the sympathetic nervous system. In the present study, the NE contents and expression levels of *Adr* did not differ significantly between the *Ctrl* and *Npy*$^{-/-}$ mice. Huan et al. (2016)[5] emphasized the ability of inflammatory cytokines such as IL-6, which are secreted from Kupffer cells in response to noradrenergic stimuli, to promote HCC growth. The results of our present investigation do not simply indicate an activation of hepatic inflammation by the loss of Npy; we observed that the IL-6-mRNA expression levels were significantly upregulated in the *Npy*$^{-/-}$-AL mice. Inflammatory or oxidative stress activates NF-κB and ERK signaling, which are reported to be associated with hepatocarcinogenesis.[14-16] However, in our present study, the phosphorylated and thus active forms of NF-κB and ERK1/2 did not differ significantly between the *Ctrl* and *Npy*$^{-/-}$ mice in the AL and HFD conditions. Our findings may thus imply the presence of direct actions of norepinephrine in HCC cells, not limited to the effects of cytokines or NF-κB or ERK1/2. In fact, norepinephrine is known to promote cancer cell migration and invasion in multiple types of cancer via Adrβ signaling.[21] The inhibition of monoamine oxidase A, a catecholamine neurotransmitter-degrading enzyme, also promotes the metastasis of HCC.[22] However, we could not find any characteristic findings of vascular invasion or poor differentiation of HCC in this study (data not shown) . Further study should be required to elucidate the relationship between SNS and hepatocarcinogenesis. Additionally, HCC is well known to be the tumor with abundant arterial blood supply. Because Npy has strong vasoconstrictive effect,[23] the growth of HCC might be accelerated in *Npy*$^{-/-}$ mice in this study.

Our present data clearly demonstrated that the long-term diet restriction (DR) significantly inhibited hepatocarcinogenesis in mice without the *Npy* gene. DR significantly inhibited steatosis and steatohepatitis even in the *Npy*$^{-/-}$ mice, supporting the current paradigm of the NAFLD and HCC sequence. However, the *Npy*$^{-/-}$-DR mice exhibited peculiar findings at 28 wks; i.e., an increased HCC cell proliferation rate compared to that of the *Npy*$^{-/-}$-AL mice, and elevated *TNFα*-mRNA levels and an increased ratio of p-NF-κB to NF-κB compared to the *Ctrl*-DR mice. It was reported that TNFα activates NF-κB signaling[24] and the activation of NF-κB in mouse liver was mostly protective against HCC.[16,25] The present results may imply that DR-associated protective mechanisms are initiated even if genotoxic or carcinogenic stress is elevated in *Npy*$^{-/-}$-DR mice. Indeed, the densities of PCNA+ and γH2AH+ cells were increased in the livers of *Npy*$^{-/-}$-DR mice at 28 wks (Suppl. Fig. S8A-C).

Nrf2 and FoxO1 transcription factors are reported to be required for the inhibiting effect of dietary restriction on tumorigenesis.[9,17] Although multiple factors could be involved in the regulation of the transcription of FoxO1 and Nrf2 target genes, the present data suggest that the deficiency of Npy affects those expression levels in the liver, implying a deregulation of the homeostasis between carcinogenic stresses and defense mechanisms. Finally, our hypothetic scheme on an association of Npy with hepatocarcinogenesis is shown in Figure 8. The Npy-Y receptor system is complex network, but currently, Yang et al. reported the structural basis of

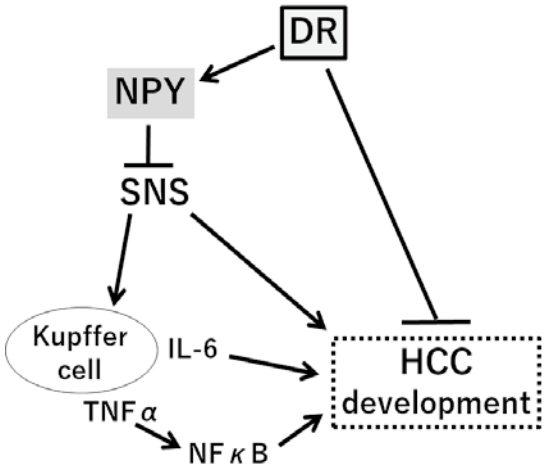

Figure 8. Hypothetic scheme of the effect of DR and Npy on the development of HCC according to this study. The arrow indicates the activation, while the bar is shown as the suppressive effect.

ligand binding modes at the Npy Y1 receptor,[26] so that it is expected to develop more effective agonist/antagonist to control obesity or carcinogenesis.

In summary, our findings establish a significant role for Npy in hepatocarcinogenesis, particularly in overnutrition. The activation of Npy signaling may be a promising target for the prevention of HCC in humans.

Acknowledgements

We thank the staff at the Laboratory Animal Center for Biomedical Research at the Center for Frontier Life Sciences at Nagasaki University for the animal care, and the Biomedical Research Support Center, Nagasaki University School of Medicine for the technical assistance. This study was supported by Grants-in-Aid for Scientific Research from the Japan Society for the Promotion of Science (JSPS; nos. 15390128, 16790226, and 20790260).

References

1. Younes R, Bugianesi E. Should we undertake surveillance for HCC in patients with NAFLD? *J Hepatol*. 2018;68:326-34.
2. Chida Y, Sudo N, Kubo C. Does stress exacerbate liver diseases? *J Gastroenterol Hepatol*. 2006;21:202-8.
3. Farzi A, Reichmann F, Holzer P. The homeostatic role of neuropeptide Y in immune function and its impact on mood and behaviour. *Acta Physiol (Oxf)*. 2015;213:603-27.
4. Sigala B, McKee C, Soeda J, et al. Sympathetic nervous system catecholamines and neuropeptide Y neurotransmitters are upregulated in human NAFLD and modulate the fibrogenic function of hepatic stellate cells. *PLoS ONE*. 2013;8:e72928.
5. Huan H-B, Wen X-D, Chen X-J, et al. Sympathetic nervous system promotes hepatocarcinogenesis by modulating inflammation through activation of alpha1-adrenergic receptors of Kupffer cells. *Brain Behav Immun*. 2016;59:118-34.
6. Weindruch R, Walford RL. The retardation of aging and disease by dietary restriction. Springfield, IL: Charles C Thomas; 1988.
7. Mattison JA, Roth GS, Beasley TM, et al. Impact of caloric restriction on health and survival in rhesus monkeys from the NIA study. *Nature*. 2012;489:318-21.
8. Chiba T, Tamashiro Y, Park D, et al. A key role for neuropeptide Y in lifespan extension and cancer suppression via dietary restriction. *Sci Rep*. 2014;4:4517.
9. Yamaza H, Komatsu T, Wakita S, et al. FoxO1 is involved in the antineoplastic effect of calorie restriction. *Aging Cell* 2010;9:372-82.
10. Maronpot RR. Biological basis of differential susceptibility to hepatocarcinogenesis among mouse strains. *J Toxicol Pathol*. 2009;22:11–33.
11. Mori R, Tanaka K, de Kerckhove M, et al. Reduced FOXO1 accelerates skin Wound healing and attenuates scarring. *Am J Pathol*. 2014;184:2465-79.
12. Goldfarb S, Pugh TD, Koen H, He YZ. Preneoplastic and neoplastic progression during hepatocarcinogenesis in mice injected with diethylnitrosamine in infancy. *Environ Health Perspect* 1983;50:149-61.
13. Maeda S, Kamata H, Luo J-L, et al. IKKbeta couples hepatocyte death to cytokine-driven compensatory proliferation that promotes chemical hepatocarcinogenesis. *Cell* 2005;121:977-90.
14. Park EJ, Lee JH, Yu G-Y, et al. Dietary and genetic obesity promote liver inflammation and tumorigenesis by enhancing IL-6 and TNF expression. *Cell*. 2010;140:197–208.
15. Pikarsky E, Porat RM, Stein I, et al. NF-kappaB functions as a tumour promoter in inflammation-associated cancer. *Nature*. 2004;431:461-6.
16. Gehrke N, Wörns MA, Mann A, et al. Hepatic B cell leukemia-3 suppresses chemically-induced hepatocarcinogenesis in mice through altered MAPK and NF-κB activation. *Oncotarget*. 2017;8:56095-109.
17. Pearson KJ, Lewis KN, Price NL, et al. Nrf2 mediates cancer protection but not prolongevity induced by caloric restriction. *Proc Natl Acad Sci USA* 2008;105:2325-30.
18. Lv X, Zhao F, Huo X, et al. Neuropeptide Y1 receptor inhibits cell growth through inactivating mitogen-activated protein kinase signal pathway in human hepatocellular carcinoma. *Med Oncol*. 2016;33:70.
19. Michalkiewicz M, Knestaut KM, Bytchkova EY, Michalkiewicz T. Hypotension and reduced catecholamines in neuropeptide Y transgenic rats. *Hypertension*. 2003;41:1056-62.
20. Baldock PA, Lin S, Zhang L, et al. Neuropeptide y attenuates stress-induced bone loss through suppression of noradrenaline circuits. *J Bone Miner Res*. 2014;29:2238-49.
21. Schler HM. Neurotransmitter Receptor-Mediated Signaling Pathways as Modulators of Carcinogenesis. Zänker KS, Entschladen F (eds): Neuronal Activity in Tumor Tissue. Prog Exp Tumor Res. Basel, Switzerland: Karger, 2007, vol. 39, pp. 45-63.
22. Li J, Tang XM, Wang YH, et al. Monoamine oxidase A suppresses hepatocellular carcinoma metastasis by inhibiting the adrenergic system and its transactivation of EGFR signaling. *J Hepatology*. 2014;60:1225-34.
23. Herring N, Tapoulal N, Kalla M, et al; Oxford Acute Myocardial Infarction (OxAMI) Study. Neuropeptide-Y causes coronary microvascular constriction and is associated with reduced ejection fraction following ST-elevation myocardial infarction. *Eur Heart J*. 2019;40:1920-29.
24. Ozes ON, Mayo LD, Gustin JA, et al. NF-kappaB activation by tumour necrosis factor requires the Akt serine-threonine kinase. *Nature*. 1999; 401:82-85.
25. Zoller H, Tilg H. Nonalcoholic fatty liver disease and hepatocellular carcinoma. *Metab Clin Exp*. 2016;65:1151-60.
26. Yang Z, Han S, Keller M, et al. Structural basis of ligand binding modes at the neuropeptide Y Y_1 receptor. *Nature*. 2018;556:520-4.

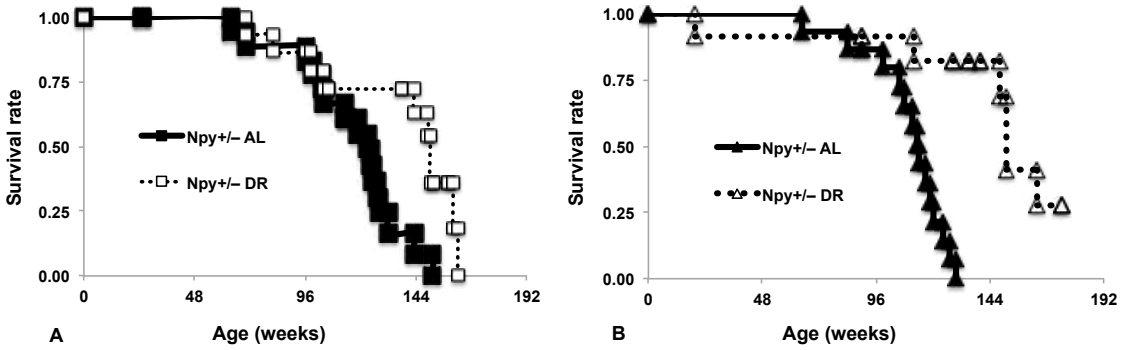

Suppl. Fig. S1. Kaplan-Meier Survival curves in male *Npy*$^{+/-}$ A: and female *Npy*$^{+/-}$ mice B: Mice were fed ad libitum (AL) or 30% dietary-restricted (DR) chow starting at 12 weeks of age. The initial numbers of mice were as follows: male *Npy*$^{+/-}$-AL (n=19) and male *Npy*$^{+/-}$-DR (n=15); Female *Npy*$^{+/-}$-AL (n=15) and female *Npy*$^{+/-}$-DR (n=12). Comparisons of survival curves by log-rank test: p=0.0078 for male *Npy*$^{+/-}$-AL vs. -DR; p=0.0001 for female *Npy*$^{+/-}$-AL vs. -DR. The details of the lifespan study were as described.[1]

Suppl. Table S1. The numbers of mice bearing tumor (Tumor +) at death

	Tumor +	–	Total
Npy$^{+/-}$-AL	23	7	33
Npy$^{+/-}$-DR	10*	11	22

The data are from the pathological analyses of the 72-wks survivor cohort (the male and female mice were combined). The proportion of mice with a tumor was significantly lower in the *Npy*$^{+/-}$-DR group than in the *Npy*$^{+/-}$-AL group, *p=0.0327. The details of pathological analysis in the lifespan study were as described.[1]

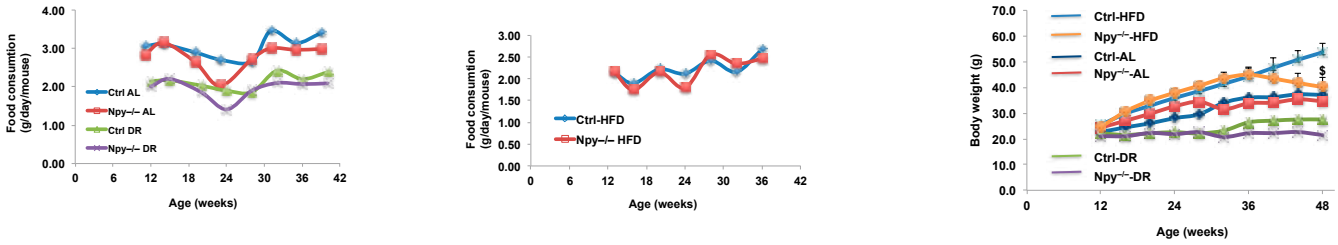

Suppl. Fig. S2. Food consumption in the experimental mice. A: Mice fed a standard diet (CRF-1; Oriental Yeast Co., Tsukuba, Japan: 357 kcal/100g). **B:** Mice fed a high-fat diet (HFD, F2HFD1 diet, Oriental Yeast Co.: 414 kcal/100 g). The composition of the CRF-1 diet was as follows (per 100 g; 357 kcal): 21.9 g protein, 5.4 g fat, 6.3 g mineral mix, 2.9 g fiber, 55.3 g nitrogen-free water-soluble substance, and 8.2 g water. The composition of the HFD was as follows (per 100 g): 7.5 g cacao butter, 1.25 g cholesterol, 0.5 g cholic acid sodium salt, 7.5 g milk casein, 1.25 g cellulose, 1.0 g vitamin mix, 1.0 g mineral mix, 1.625 g sucrose, 1.625 g glucose, 1.625 g dextrin, 0.125 g choline chloride, 72 g CRF-1, and 3 g lard. The body weight of all mice was monitored every 4 weeks. The standard diet (CRF-1) consumption of the *Npy*$^{-/-}$-AL mice was approx. 9% lower than that of the *Ctrl*-AL mice during the experiment (Suppl. Fig. 2A). Hence, the daily allotments for the DR groups, which were adjusted to 70% of the dietary intakes of the individual AL groups, were also lower in the *Npy*$^{-/-}$-DR mice compared to the *Ctrl*-DR mice. The food intake of the HFD groups did not significantly differ between the *Ctrl* and *Npy*$^{-/-}$ mice (Suppl. Fig. 2B). The food consumption data were collected from 3–5 cages. **C: The body weights (BWs) in the experimental mice.** The BWs did not significantly differ between the *Ctrl*-AL and *Npy*$^{-/-}$-AL mice (Fig. 1). The BWs of the *Npy*$^{-/-}$-DR mice were almost the same as those of the *Ctrl*-DR mice between 12 and 24 wks, whereas between 28 wks and 48 wks the BWs were 11%-21% lower in the *Npy*$^{-/-}$-DR mice compared to the *Ctrl*-DR mice. The BWs in the *Ctrl*-HFD group progressively increased between 12 and 48 wks. The BWs in the *Npy*$^{-/-}$-HFD mice increased until 32 wks and then decreased. Consequently, the BWs at 48 wks tended to be lower in the *Npy*$^{-/-}$ HFD mice compared to the *Ctrl*-HFD mice (p=0.0685).

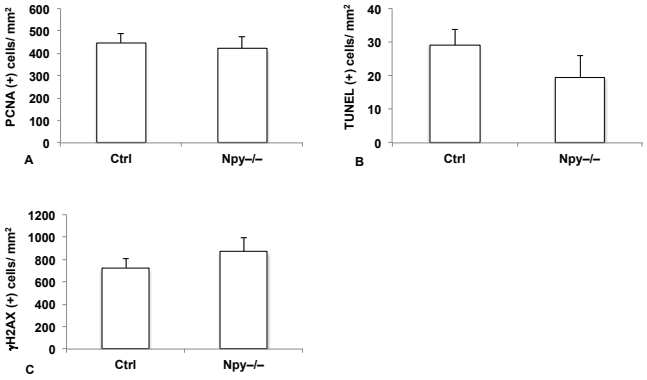

Suppl. Fig. S3. The densities of PCNA+ (**A**), TUNEL+ (**B**), and gannma γH2AX+ hepatocytes (**C**) in the liver 48 hr after DEN administration to mice at 15 days of age. The data are mean ± SE of four *Ctrl* mice and five *Npy*$^{-/-}$ mice.

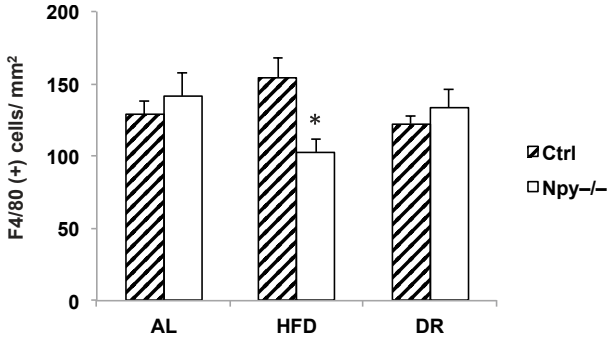

Suppl. Fig. S4. The density of F4/80+ cells in the liver. *p<0.05 vs. *Ctrl*-HFD. The data are mean ± SE of six mice in each group.

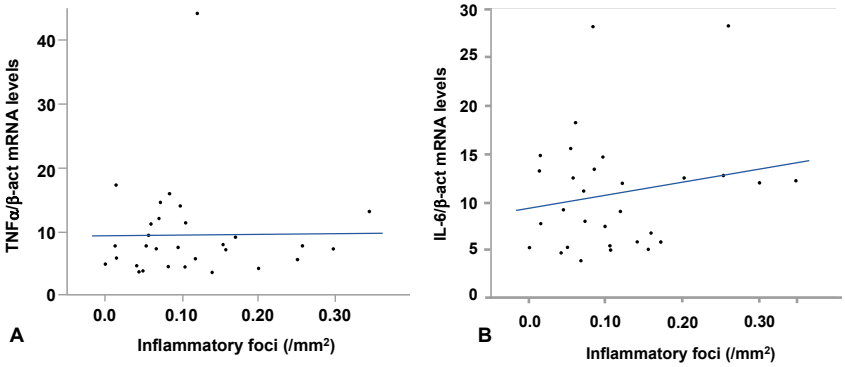

Suppl. Fig. S5. Correlation between cytokine mRNA expression levels and the density of hepatic inflammatory foci. A: TNFα/β -act mRNA. **B:** IL-6/β-act mRNA.

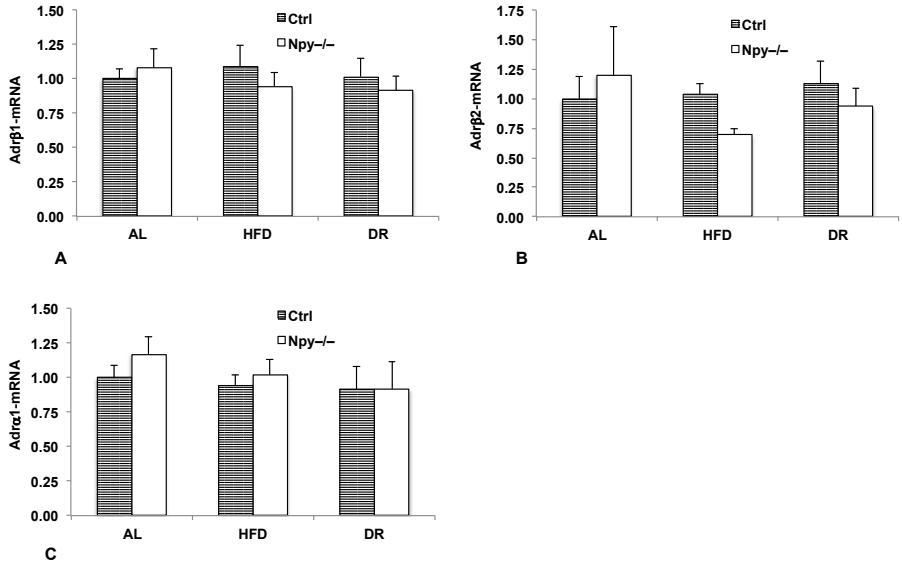

Suppl. Fig. S6. The mRNA expression levels of adrenergic receptors. The levels were normalized by β-actin mRNA levels. **A:** Adrenergic receptor β1. **B:** Adrenergic receptor β2. **C:** Adrenergic receptor α1. Bars: mean ± SE (n=6). Neither the genotype nor the dietary regimens affected the mRNA expression levels of these adrenergic receptor subtypes.

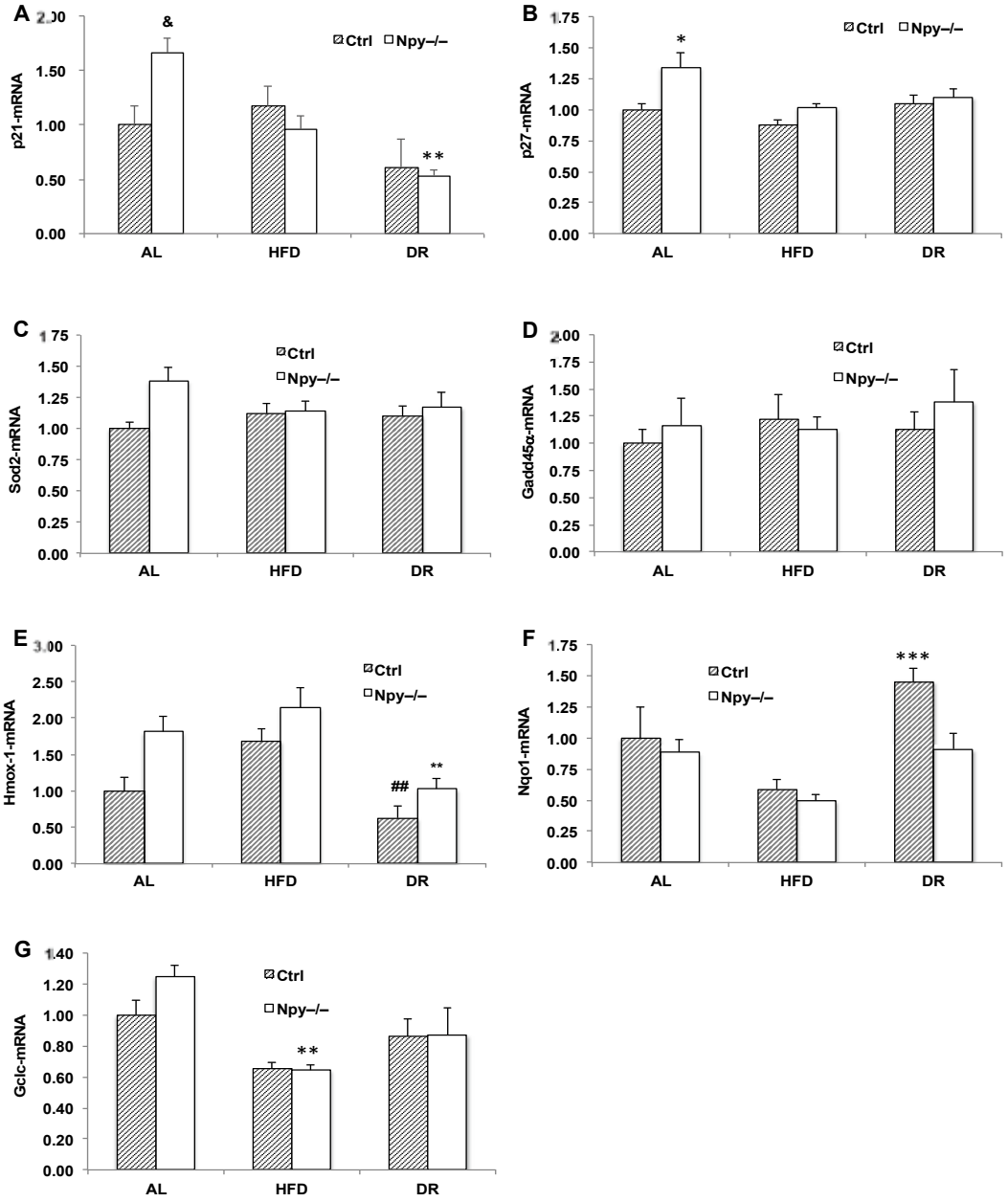

Suppl. Fig. S7. The expression levels of mRNA in the liver at 28 wks. Each gene level was normalized by the β-actin-mRNA level. **A:** p21-mRNA levels. $^{\&}$p=0.0913 vs. *Ctrl*-AL. **p=0.0013 vs. *Npy*$^{-/-}$-AL. **B:** p27-mRNA levels. *p=0.0194 vs. *Ctrl*-AL. **C:** Sod2-mRNA levels. $^{\$}$p=0.0622 vs. *Ctrl*-AL. **D:** Gadd45α-mRNA levels. **E:** Hmox-1-mRNA expression levels. **p=0.0044 vs. Ctrl-HFD. $^{\#\#}$p=0.0075 vs. *Npy*$^{-/-}$-DR. **F:** Nqo-1-mRNA levels. ***p=0.0009 vs. *Ctrl*-HFD. $^{\$}$p=0.0686 vs. *Npy*$^{-/-}$-DR. **G:** Gclc-mRNA levels. **p=0.0032 vs. *Npy*$^{-/-}$-AL.

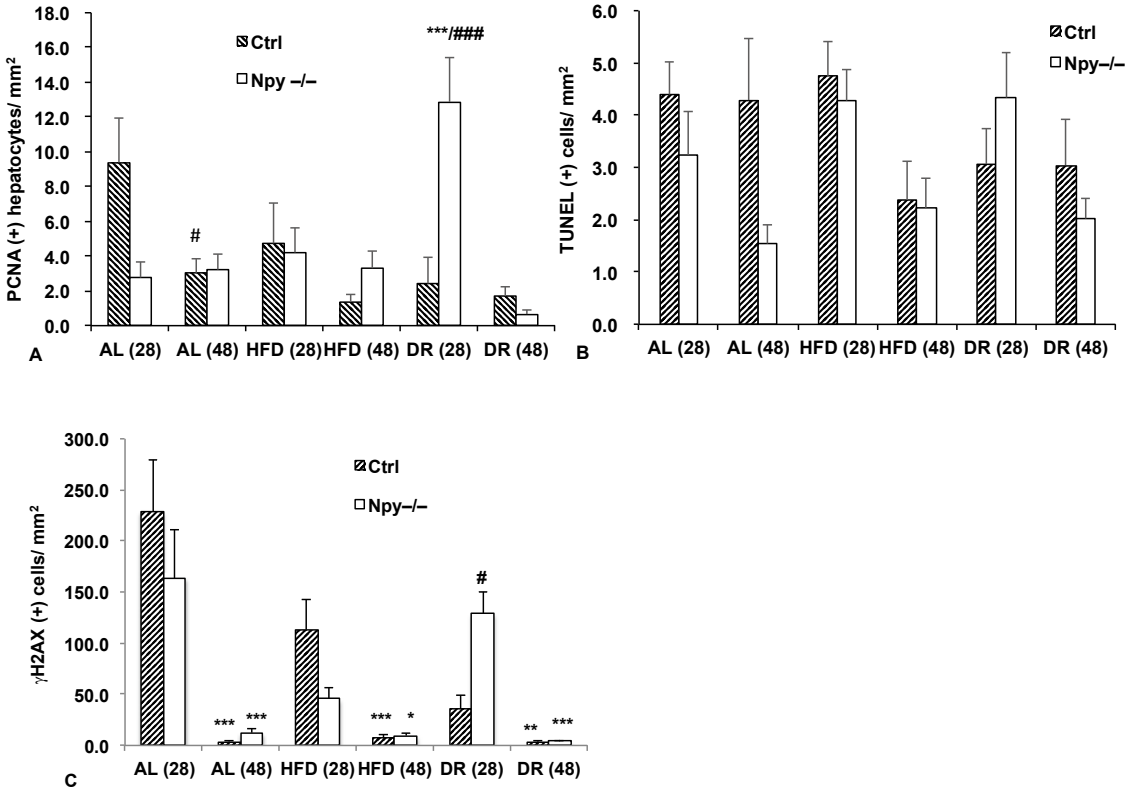

Suppl. Fig. S8. Cell proliferation, death, and DNA damage in hepatocytes. A: The density of PCNA+ hepatocytes at 28 and 48 wks. $^{\#}$p=0.0382 vs. *Ctrl*-AL (28 wks). ***p<0.0001 vs. *Ctrl*-DR (28 wks), $^{\#\#\#}$p<0.0001 vs. $Npy^{-/-}$-DR (48 wks). **B:** The density of TUNEL+ hepatocytes. **C:** The density of gH2AX+ hepatocytes. In the AL groups, ***p<0.0001 vs. *Ctr*l-AL (28 wks) and $Npy^{-/-}$-DR (28 wks). In the HFD group, ***p<0.0001 vs. *Ctrl*-HFD (28 wks), *p=0.0107 vs. $Npy^{-/-}$-HFD (28 wks). In the DR group, $^{\#}$p=0.0266 vs. *Ctrl*-DR (28 wks), **p=0.0054 vs. *Ctrl*-DR (28 wks), ***p<0.0001 vs. $Npy^{-/-}$-DR (28 wks).

Hepatic tissue milieus affected by the loss of *Npy* and the diets may modulate cell proliferation, cell death, and DNA damage in non-neoplastic hepatocytes in a manner similar to that in HCC cells. Here, the PCNA+ hepatocyte density was reduced between 28 and 48 wks (panel A; Age, p<0.0001), although the diets affected the aging-related reduction (Age × Diet, p=0.0382). It should be noted that the PCNA+ cell density was significantly higher in the $Npy^{-/-}$-DR mice at 28 wks (vs. *Ctrl*-DR, ***p<0.0001) as in HCC cells (Fig. 2A). The aging-related reduction of PCNA+ cells was significant in the *Ctrl*-AL and $Npy^{-/-}$-DR mice ($^{\#}$p=0.0382, $^{\#\#\#}$p<0.0001, respectively). There was no such significant reduction in the other groups.

The TUNEL+ hepatocyte density was reduced between 28 and 48 wks (panel B; Age, p=0.0011). The density was somewhat low in the $Npy^{-/-}$ mice compared to the *Ctrl* mice (Genotype, p=0.0836). The diet did not affect the TUNEL+ cell density (p=0.7859).

The density of γH2AX+ cells was significantly reduced between 28 and 48 wks (panel C; Age, p<0.0001) in all groups of mice. The density was low in the DR groups compared to the AL groups (Diet, p=0.0038, AL vs. DR, p=0.0021). The density was also somewhat low in the HFD groups compared to the AL groups (AL vs. HFD, p=0.0537). It should be noted that the γH2AX+ cell density at 28 wks was significantly greater in the $Npy^{-/-}$-DR mice than in the *Ctrl*-DR mice (p=0.0266).

Supplemental Text: Western blots

For the extraction of whole tissue lysate, approx. 20 mg of frozen liver was homogenized in 0.4 mL of T-PER buffer (Thermo Fisher Scientific, Waltham, MA, USA) with a protease-inhibitor cocktail (P8340 Sigma-Aldrich, St. Louis, MO) and a phosphatase-inhibitor cocktail (Nacalai Tesque, Kyoto, Japan). The homogenates were centrifuged at 10,000×g for 15 min at 4°C, and the supernatant was collected. Protein concentrations were measured using a BCA assay kit (Thermo Fisher Scientific). All samples were mixed with Laemmli's sample buffer and heated at 95°C for 5 min. Proteins (4μg) were separated by 12.5% sodium

dodecyl sulfate-polyacrylamide gel electrophoresis (SDS-PAGE) and transferred to polyvinylidene difluoride (PVDF) membranes. The membranes were immediately placed in blocking solution (Blocking One-P: Nacalai Tesque) for 30 min at room temperature.

The primary antibodies were as follows: p-NF-κB p65 Ser536 (#3033; Cell Signaling Technology, Danvers, MA), NF-κB p65 (#8242; Cell Signaling Technology), p-p44/42 MAPK (ERK1/2) (#4370; Cell Signaling Technology), p44/42 MAPK (#4695; Cell Signaling Technology), β-actin (#ab8227; Abcam, Cambridge, UK), and Lamin B1 (#ab16048, Abcam). The membranes were incubated with each antibody diluted at 1:2,000 in immunoreaction enhancer solution (Can Get Signal® Solution 1; Toyobo, Osaka, Japan) for 16 hr at 4°C with gentle shaking, and washed three times in TBS-T. The membranes were then incubated for 1 hr with horseradish peroxidase (HRP)-conjugated anti-rabbit IgG (Cell Signaling Technology) diluted 1:10,000 in immunoreaction enhancer solution (Can Get Signal® Solution 2, Toyobo) for 1 hr at room temperature with gentle shaking, and washed three times in TBS-T.

Immunoreactive proteins were visualized using Immuno Star LD (Wako Pure Chemical Industries, Osaka, Japan) or ECL-plus (Thermo Fisher Scientific) and quantified by Fusion Solo S (Vilber Lourmat, Marne la Vallee, France) and MultiGauge software (Fujifilm, Tokyo). To minimize variations in signal intensity, a standard sample was included in each blot.

Supplemental Text: Detection of norepinephrine by ELISA

To detect the content of norepinephrine (NE) in the liver, we weighted 15 mg of mouse liver tissue from each sample, and the tissues were homogenized in 0.01 N HCl in the presence of EDTA and sodium metabisulfite on ice, followed by centrifugation for 5 min at 10,000×g. The supernatant was immediately collected for analysis. The concentration of NE was measured using a norepinephrine enzyme-linked immunosorbent assay (ELISA) kit (Abnova, Taoyuan City, Taiwan). All samples were extracted using an extraction plate under shaking for 60 min at room temperature (20°-25°C) and incubated with acylation buffer. The NE ELISA was then performed according to the manufacturer's instructions. All samples were added in order to each well of the Microtiter Plate strips and then incubated with catechol-O-methyltransferase for 2 hr at 37°C. Each sample was evaluated in duplicate. The supernatants were transferred to Noradrenaline Microtiter Strips and incubated with NE antiserum overnight at 4°C. The conjugated samples were then incubated for 20-30 min, followed by incubation with the substrate solution for 30 min at room temperature (20-25°C) in the dark. The reaction was terminated using a stop solution, and the optical density was determined at 450 nm using a THERMOmax™ microplate reader (Molecular Devices, Sunnyvale, CA). The best standard curve was constructed. Based on the standard curve, we determined the NE content in each sample.

Supplemental Text: Quantitative real-time RT-PCR analysis

Amplification and real-time detection were performed using a LightCycler 480 instrument II (Roche Diagnostics, Mannheim, Germany). Each sample was analyzed in duplicate. The expression levels of the genes were normalized to those of mouse β-actin (ACTB, MA050368; TaKaRa Bio, Shiga, Japan) as an endogenous control.

Gene-specific primer sets for mRNA were obtained from the Perfect Real Time support system (TaKaRa Bio) for IL6 (MA104898), TNF-α (MA117190), NQO1 (MA086424), Hmox1 (MA089154), Gadd45a (MA095480), Gclc (MA058173), p21 (MA083344), p27 (MA099459), and SOD2 (MA031414). The other primers were as follows: ACC1 (forward, TGGCAGACCACTATGTTCCA; reverse, GTTCTGGGAGTTTCGGGTTC), PPARα (forward, ATCCACGAAGCCTACC; reverse, CACACCGTACTTTAGCAAG), Adra1a (forward, ACTGGTGATCGTGGAGTTATTGG; reverse, GGGCTCGCTTCTTGCTTCT), Adrb1 (forward, ATCTCGGCGTTGGTGTCCT; reverse, CAGCACTTGGGGTCGTTGT), Adrb2 (forward, GTCAACTCTGCCTTCAATCCTCTT; reverse, TGTAGTCCGTTCTGCCGTTG), Adrb3 (forward, ACACCCCTCCCTCTCCAAA; reverse, CCAGTCCACACACCTTTCTCC), SREBP1c (forward, TGATGCTACGGGTACACACC; reverse, TTGCGATGTCTCCAGAAGTG), LPL (forward, CTGCTGGCGTAGCAGGAAGT; reverse, GCTGGAAAGTGCCTCCATTG), HL (forward, GACGGGAAGAACAAGATTGGAA; reverse, TTGGCATCAGGAGAAAGG).

Supplemental Text References

1. Chiba T, Tamashiro Y, Park D, et al. A key role for neuropeptide Y in lifespan extension and cancer suppression via dietary restriction. *Sci Rep.*2014;4: 4517.